Type IIP Supernovae

Victor Utrobin
ITEP, Moscow

April 22, 2015

Core-Collapse Supernova Fractions

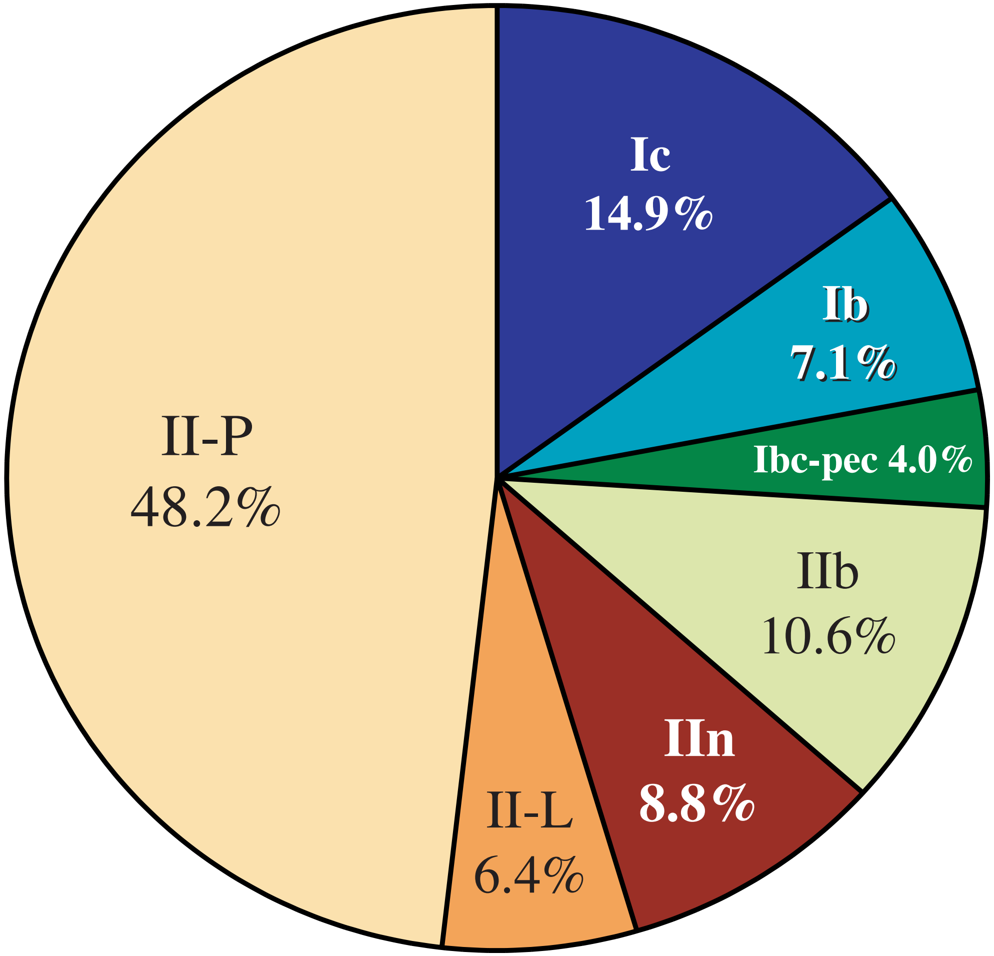

Relative fractions of core-collapse supernova types in a volume-limited sample (Smith et al. 2011).

Spectra of Type IIP Supernovae

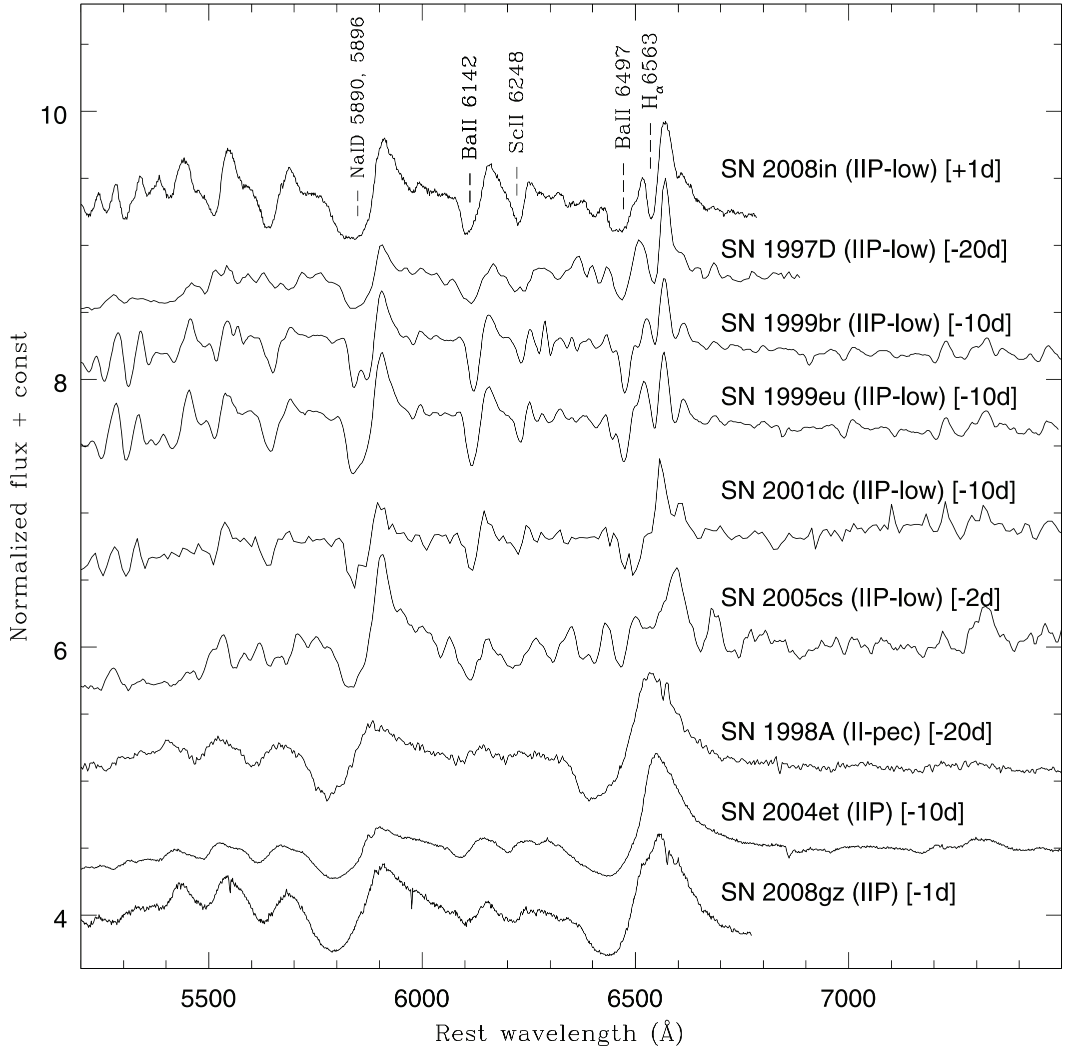

End plateau spectra of different type IIP SNe (Roy et al. 2011).

Light Curves of Type IIP Supernovae

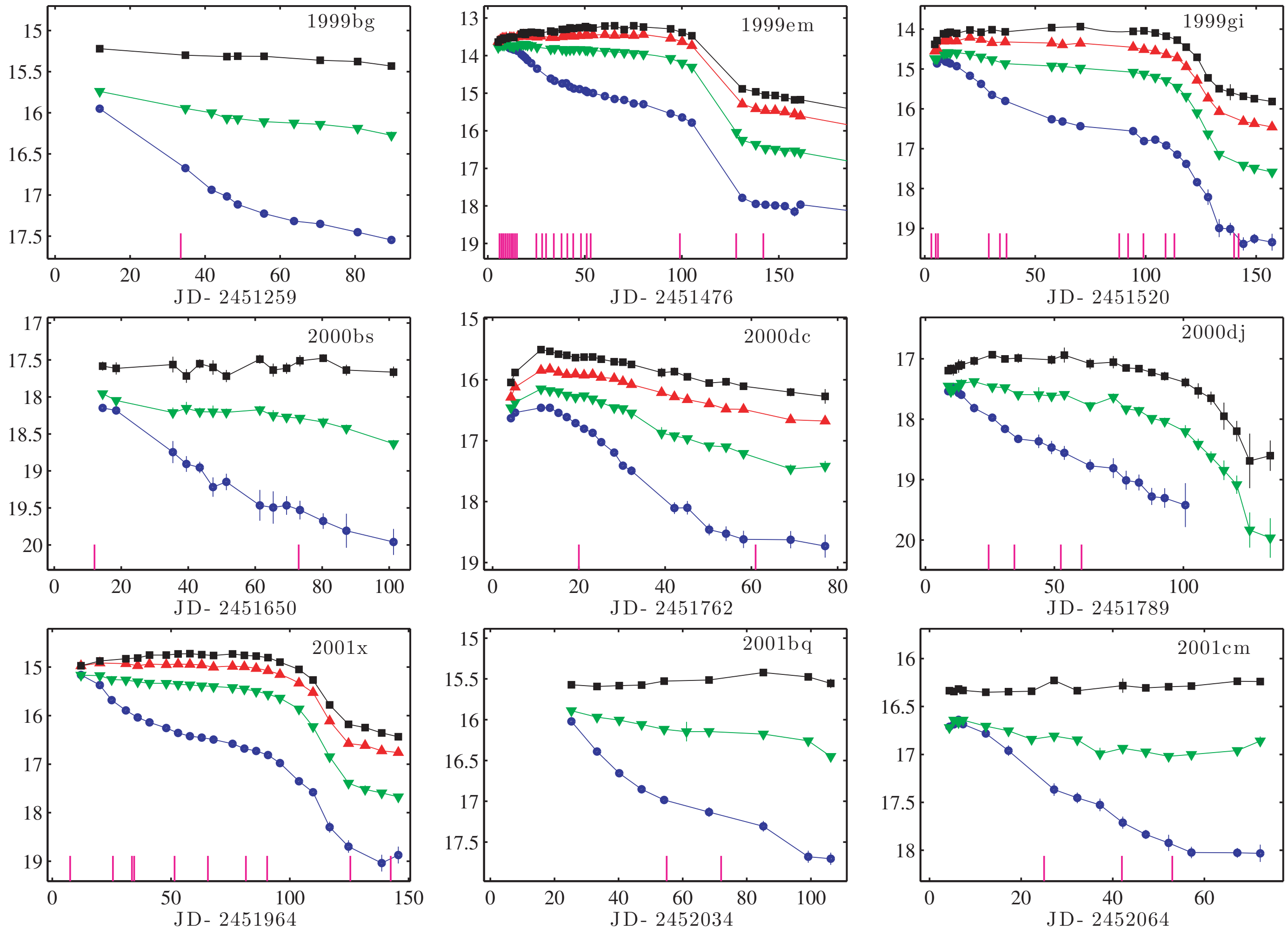

Light curves of SNe IIP: B (blue), V (green), R (red), and I (black) (Poznanski et al. 2009).

Death of Massive Stars

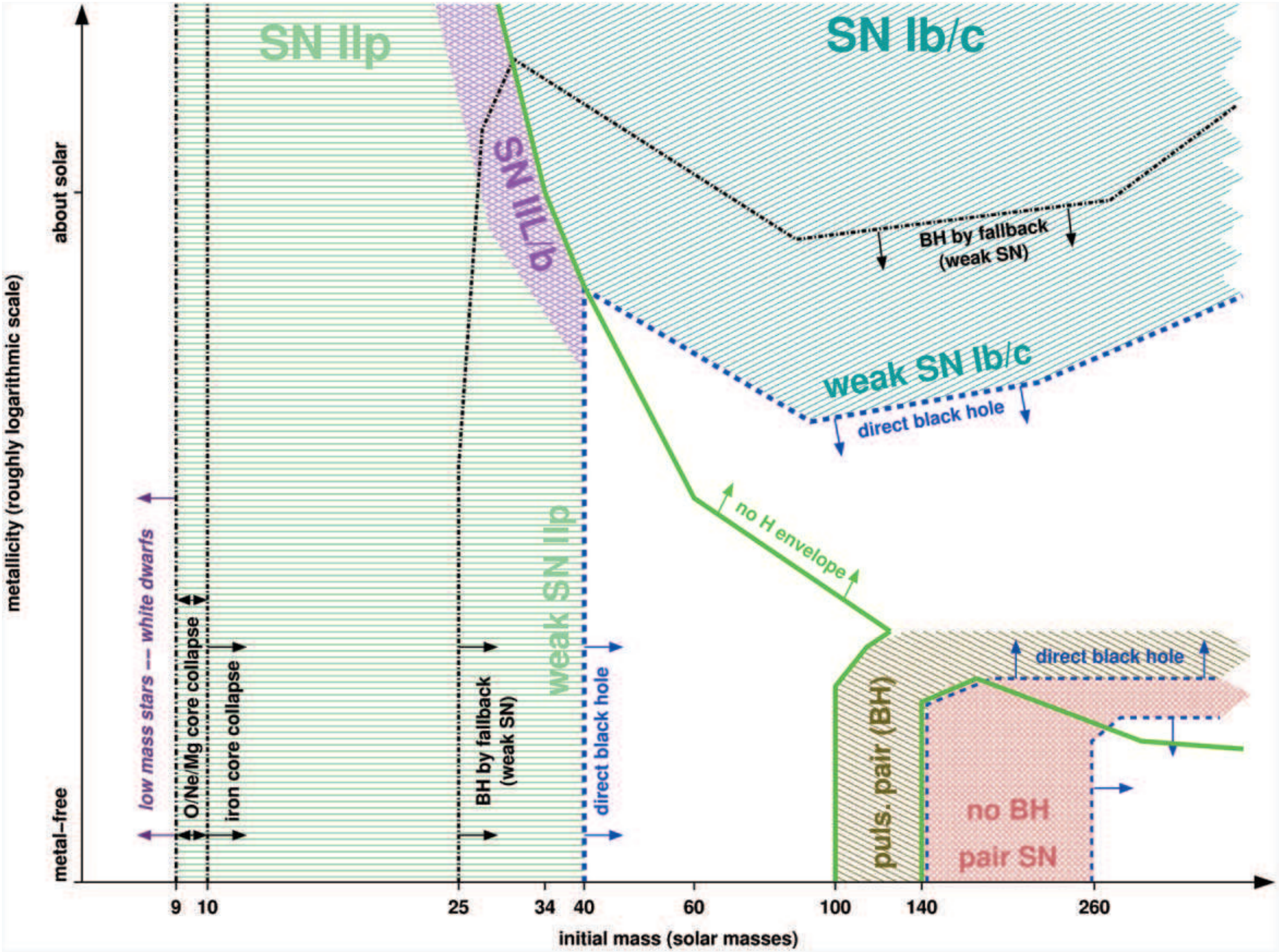

General paradigm: type IIP SNe originate from the 9–25 $M_{\odot}$ M-S stars (Heger et al. 2003).

Evolutionary tracks in the $T_c - \rho_c$ plane

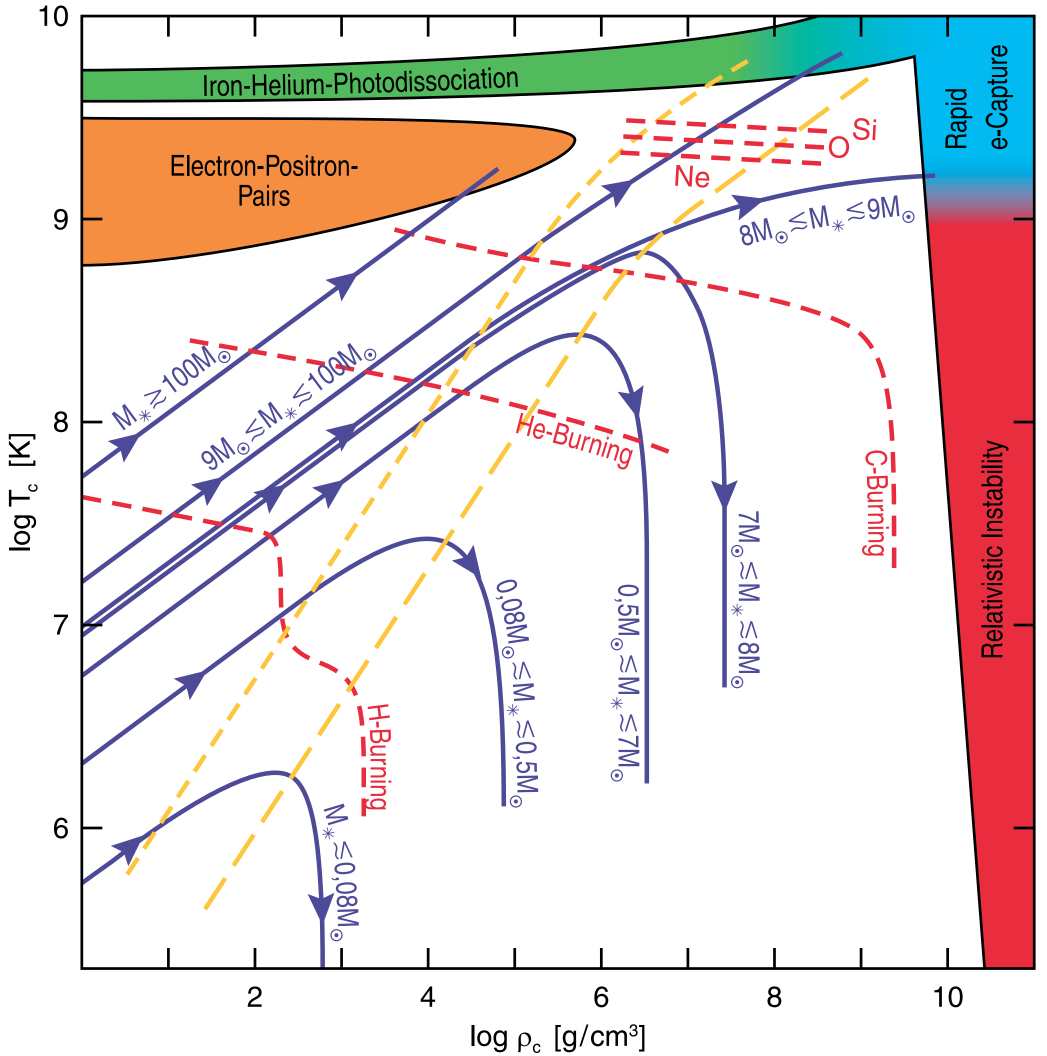

Janka (2012)

Two Methods to Estimate Mass of Progenitor Star

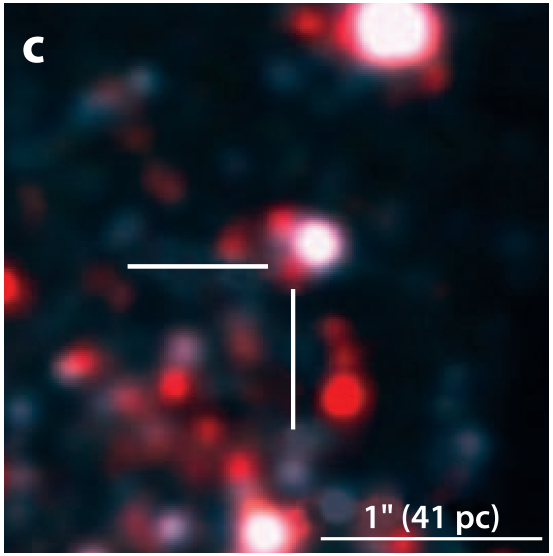

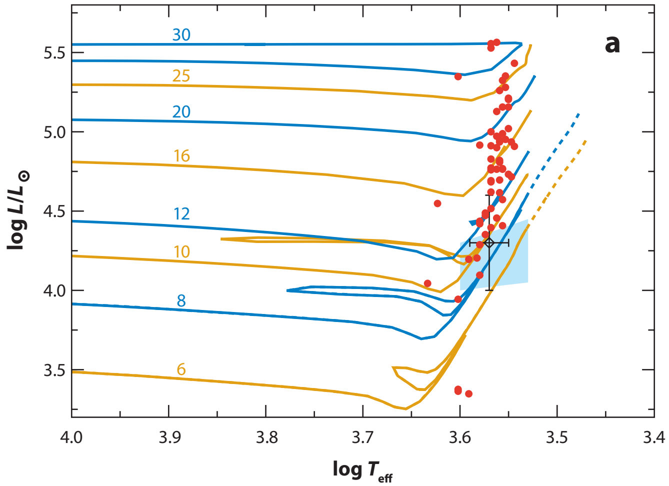

"Pre-SN image mass"
The flux and the color index of pre-SN can be converted into mass using the evolution models. It is measured for 13 pre-SNe, and for 10 the upper limits are estimated (Smartt 2009, Elias-Rosa et al. 2009, Fraser et al. 2011, 2012, Van Dyk et al. 2012, Tomasella et al. 2013).

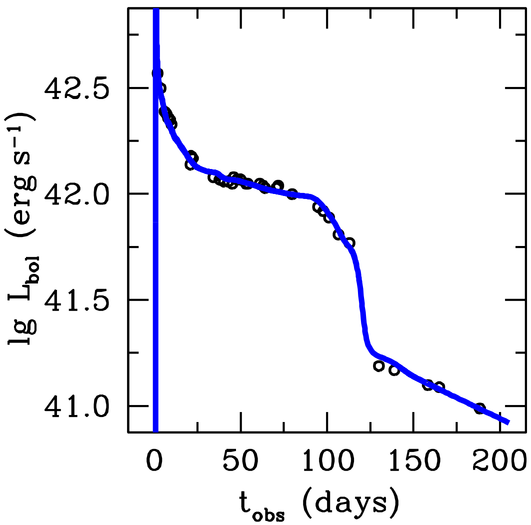

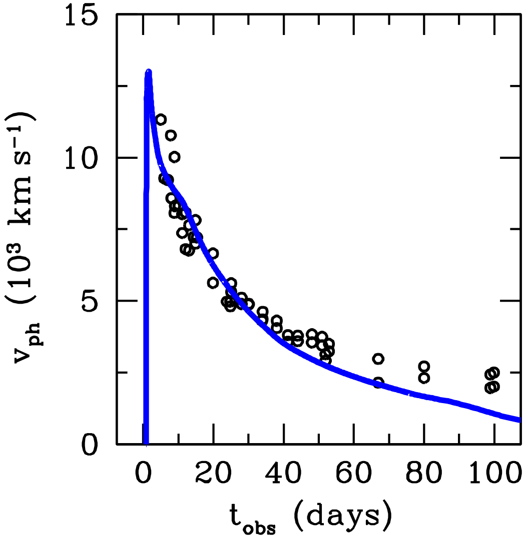

"Hydrodynamic mass"
Hydrodynamic modeling recovers the ejecta mass which, combined with the NS mass and the mass lost by stellar wind, gives the mass of a M-S star. Hydrodynamic mass is measured for 9 objects.

Positions of Detected Type II Progenitors

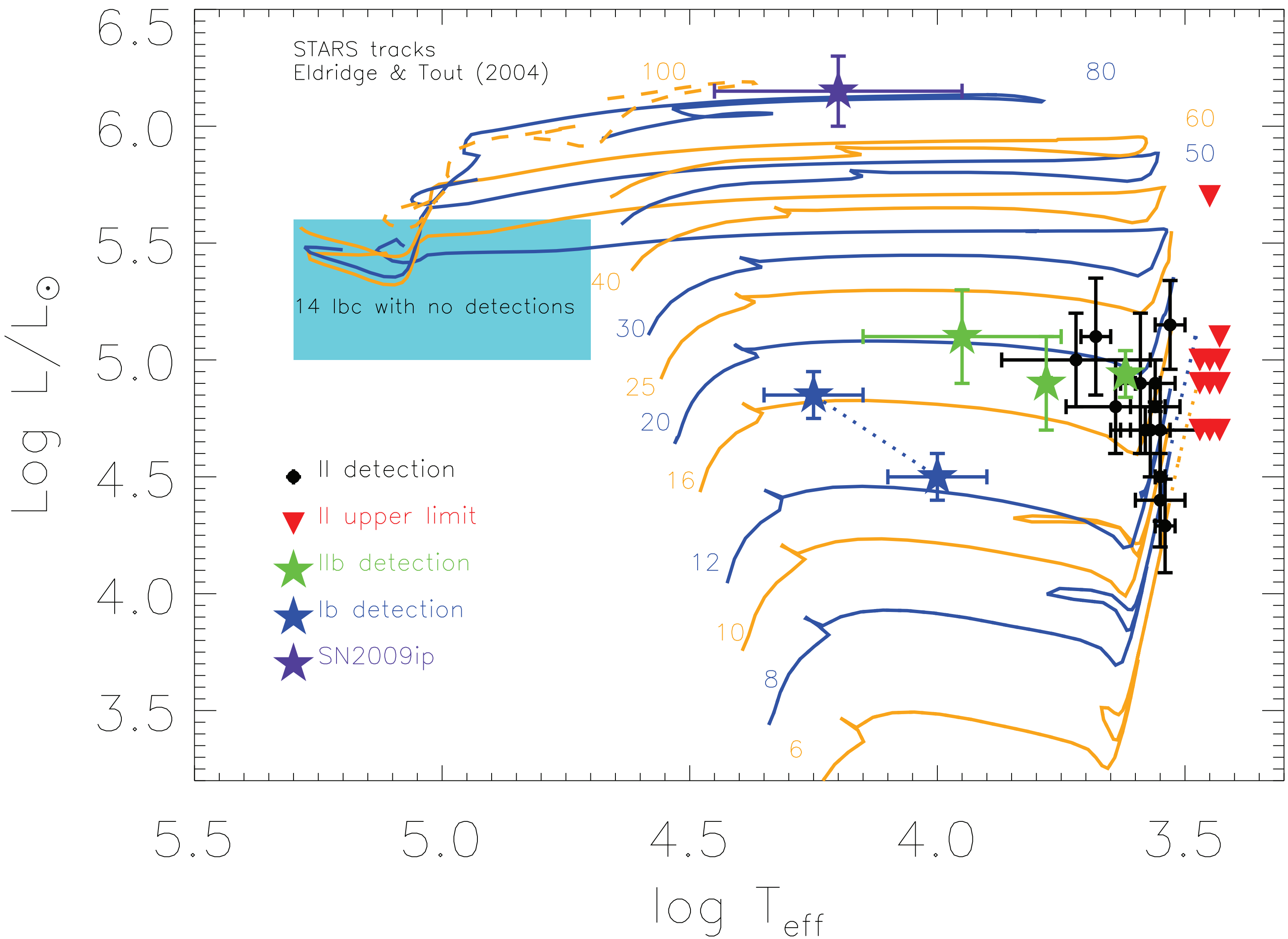

Smartt (2015)

Urgently Needed Observations of Type IIP Supernovae

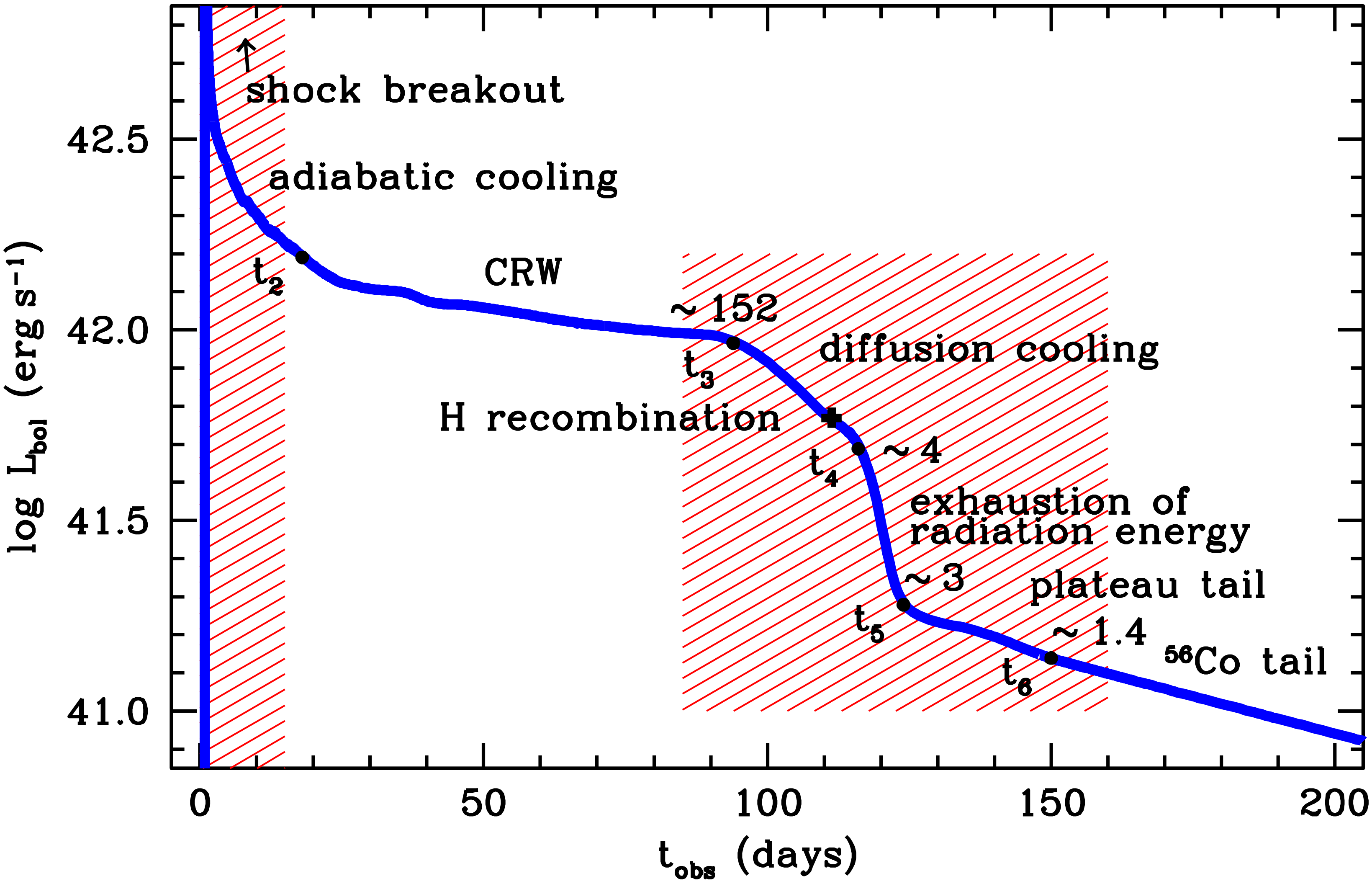

Complete photometry, good spectra, early detection, and transition from plateau to ^{56}Co tail.

Light Curves of Ordinary Type IIP Supernovae

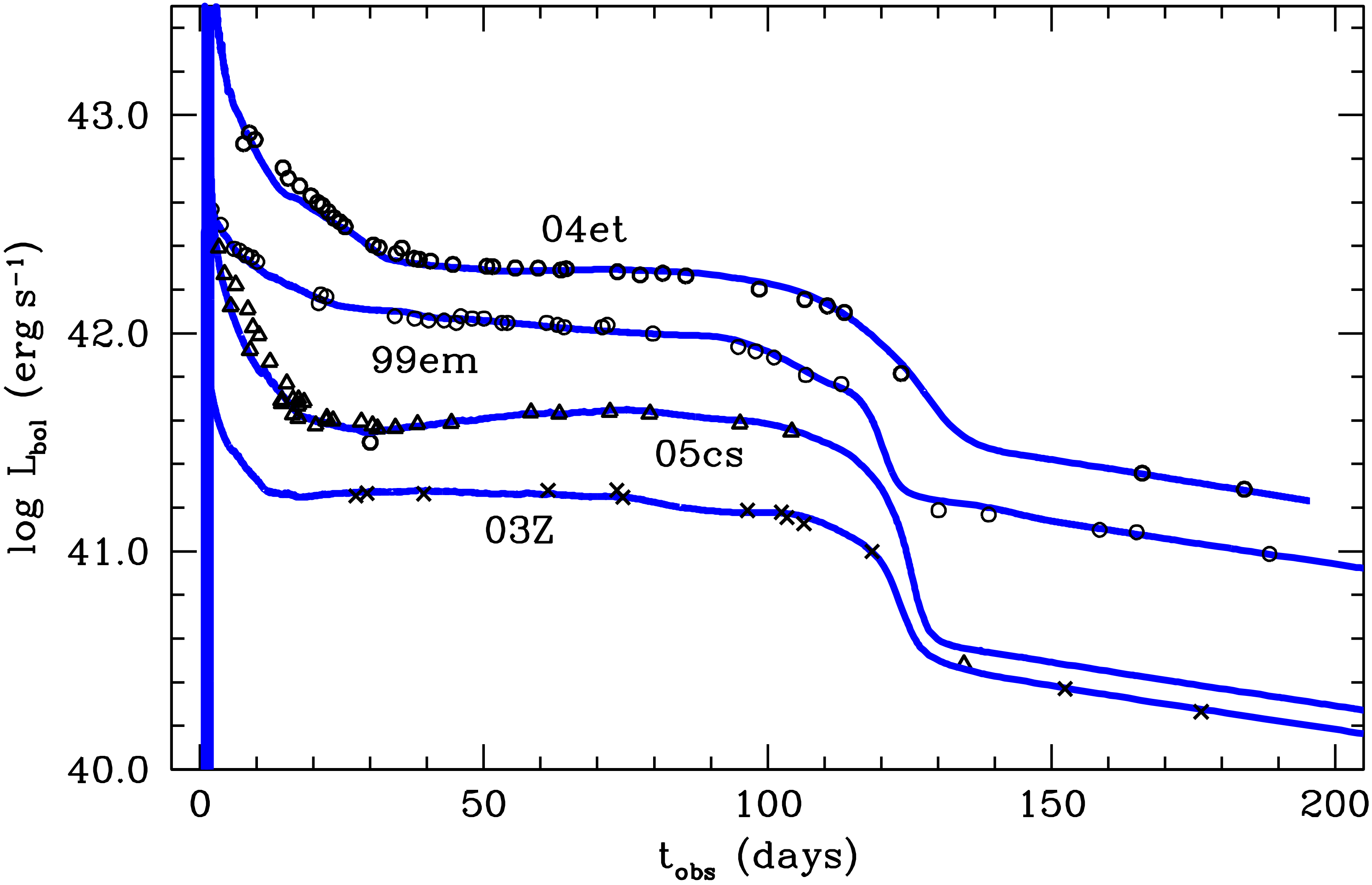

Luminosity at the plateau varies by ~ 1.2 dex for type IIP SNe which result from RSG stars.

Light Curves of Peculiar Type IIP Supernovae

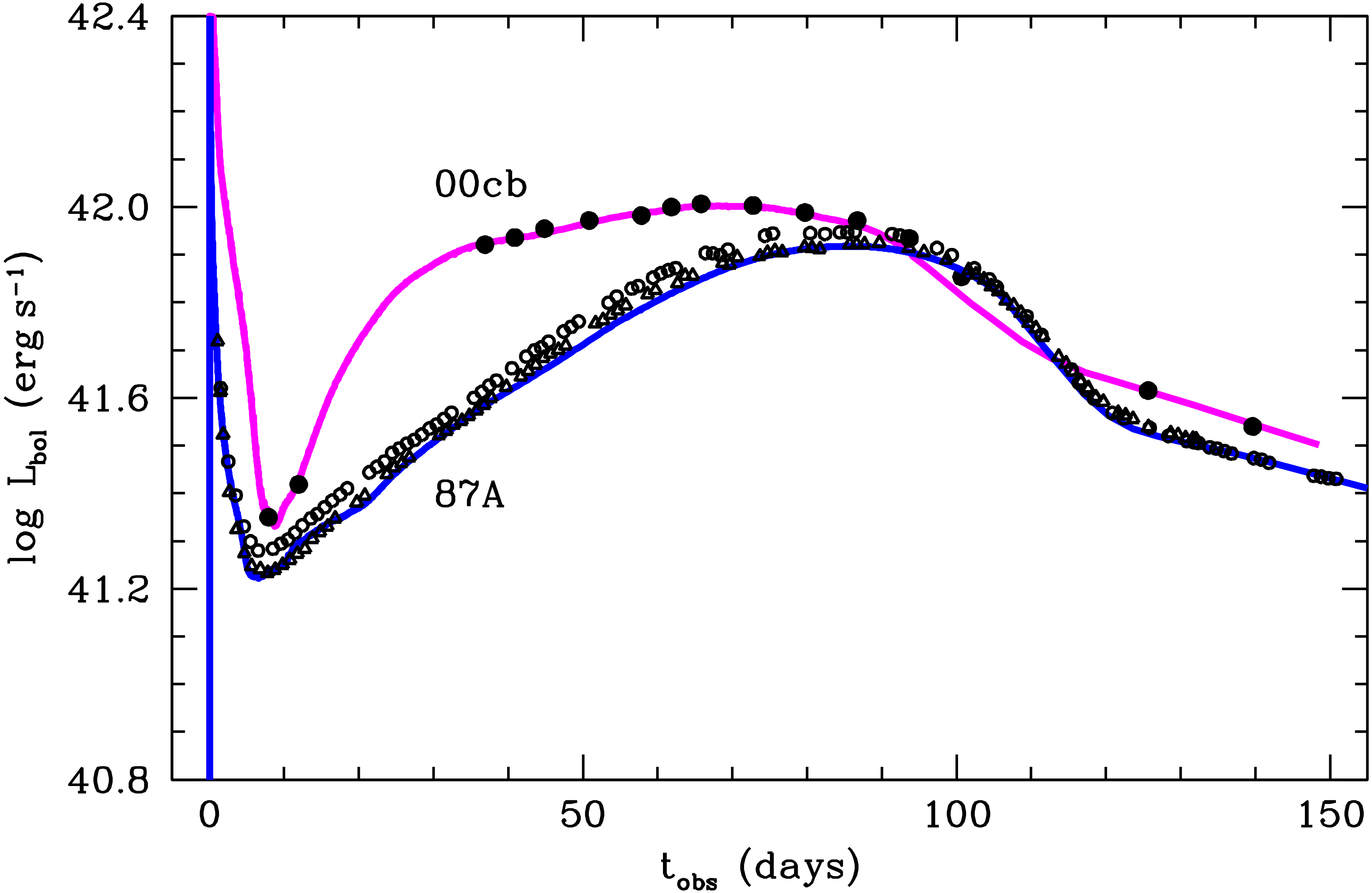

For BSG pre-SNe, the doom-like light curves are entirely powered by radioactive decay.

Hydrodynamic Models for Type IIP Supernovae

SN	R_0 ($R_\odot$)	M_{env} ($M_\odot$)	E (10^{51} erg)	$M_{\rm Ni}$ ($10^{-2} M_\odot$)	$v_{\rm Ni}^{max}$ (km s^{-1})	$v_{\rm H}^{min}$ (km s^{-1})
SN 1987A	35	18	1.5	7.65	3000	600
SN 1999em	500	19	1.3	3.60	660	700
SN 2000cb	35	22.3	4.4	8.3	8400	440
SN 2003Z	230	14	0.245	0.63	535	360
SN 2004et	1500	22.9	2.3	6.8	1000	300
SN 2005cs	600	15.9	0.41	0.82	610	300
SN 2008in	570	13.6	0.505	1.5	770	490
SN 2009kf	2000	28.1	21.5	40.0	7700	410
SN 2012A	715	13.1	0.525	1.16	710	400

- The diversity in observational data transforms into wide range of SN parameters.
- Most of type IIP pre-SNe are found to be RSGs, while two peculiar objects with dome-like light curves originate from BSGs.
- Mixing between He core and H envelope, indicated by low H velocity, is needed.
- Huge explosion energy of SN 2009kf: the sign of a **BH** formation?

Current State of Type IIP Progenitors

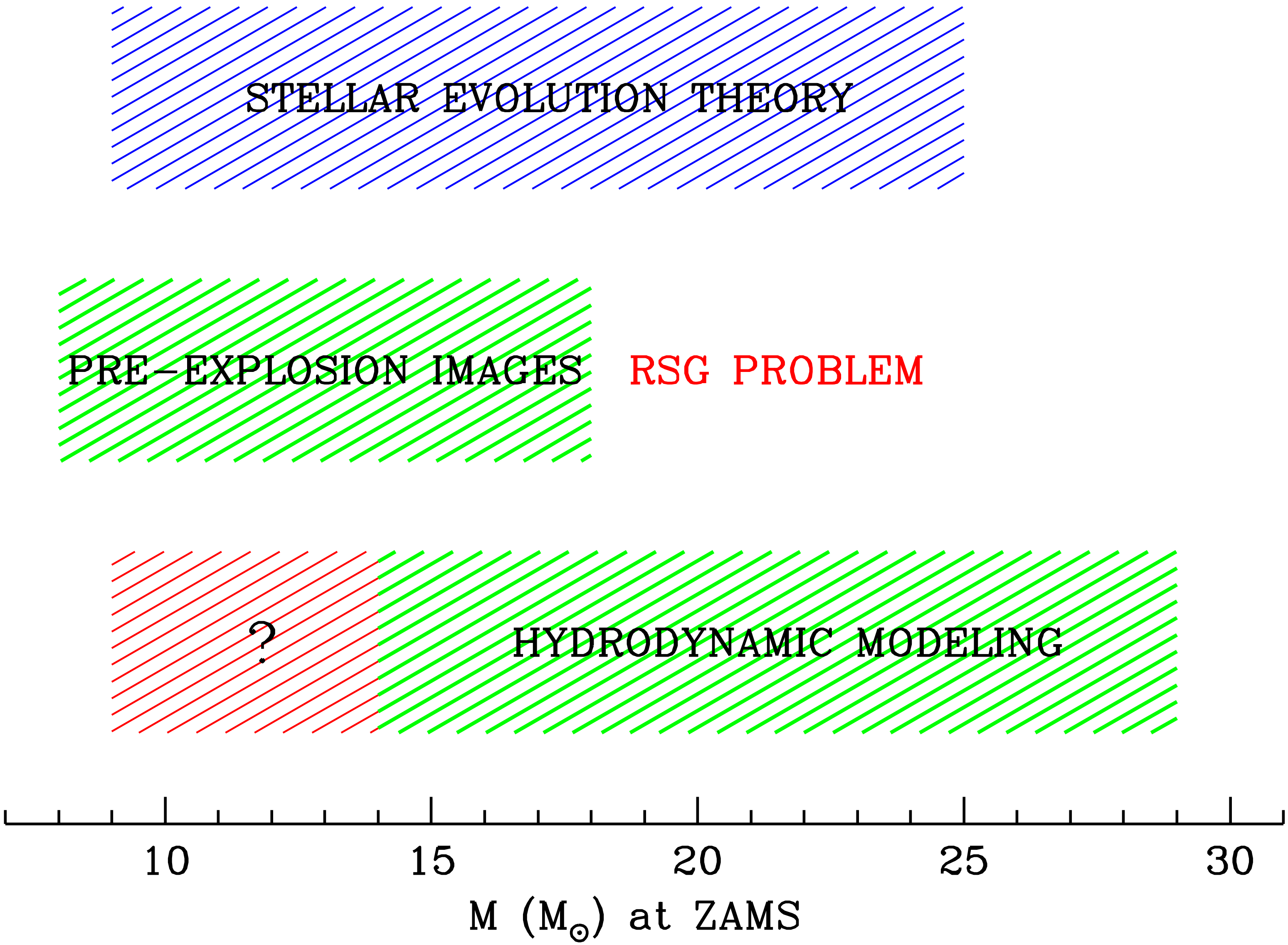

The M-S mass controversy still remains for hydrodynamic modeling.

Crucial Role of Spectral Data

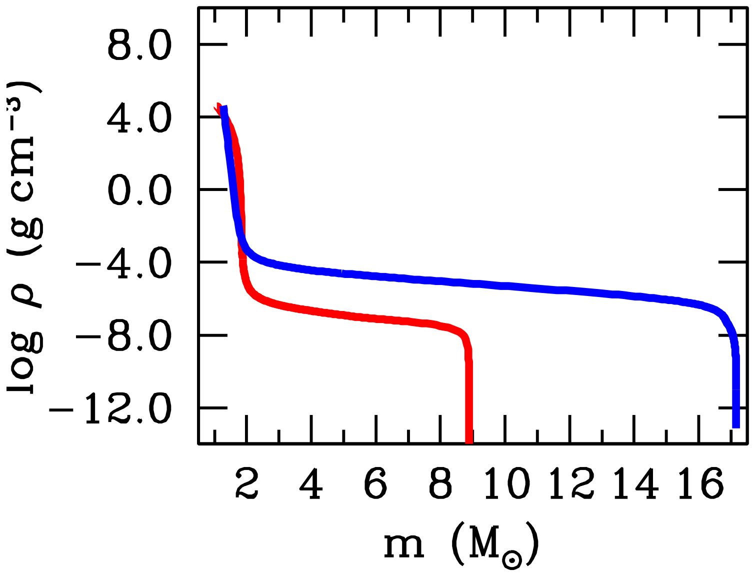

SN 2005cs

optimal / "evolutionary" model

$R_0(R_\odot) = 600/700$

$M_{env}(M_\odot) = 15.9/7.8$

$E(10^{50}\mathrm{erg}) = 4.1/1.4$

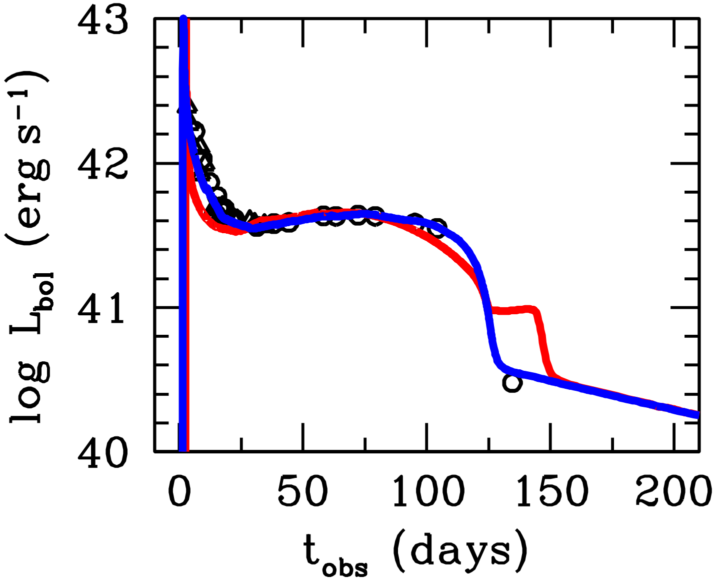

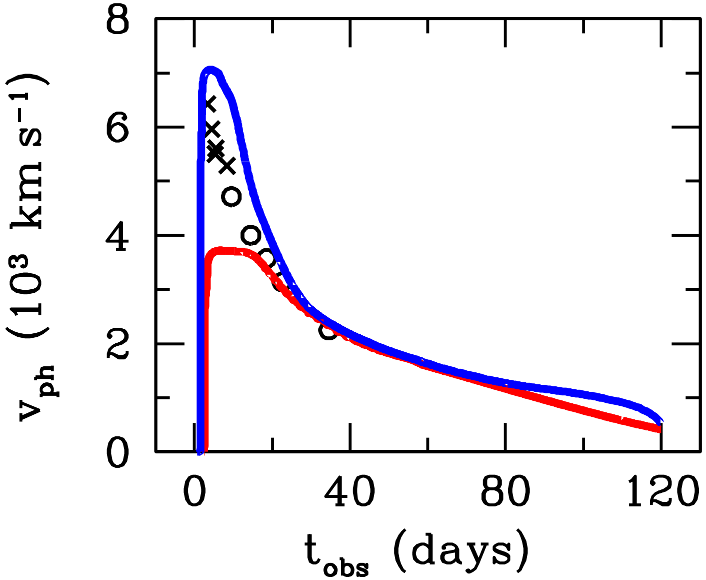

Time-Dependent Effects in Photospheric Spectra

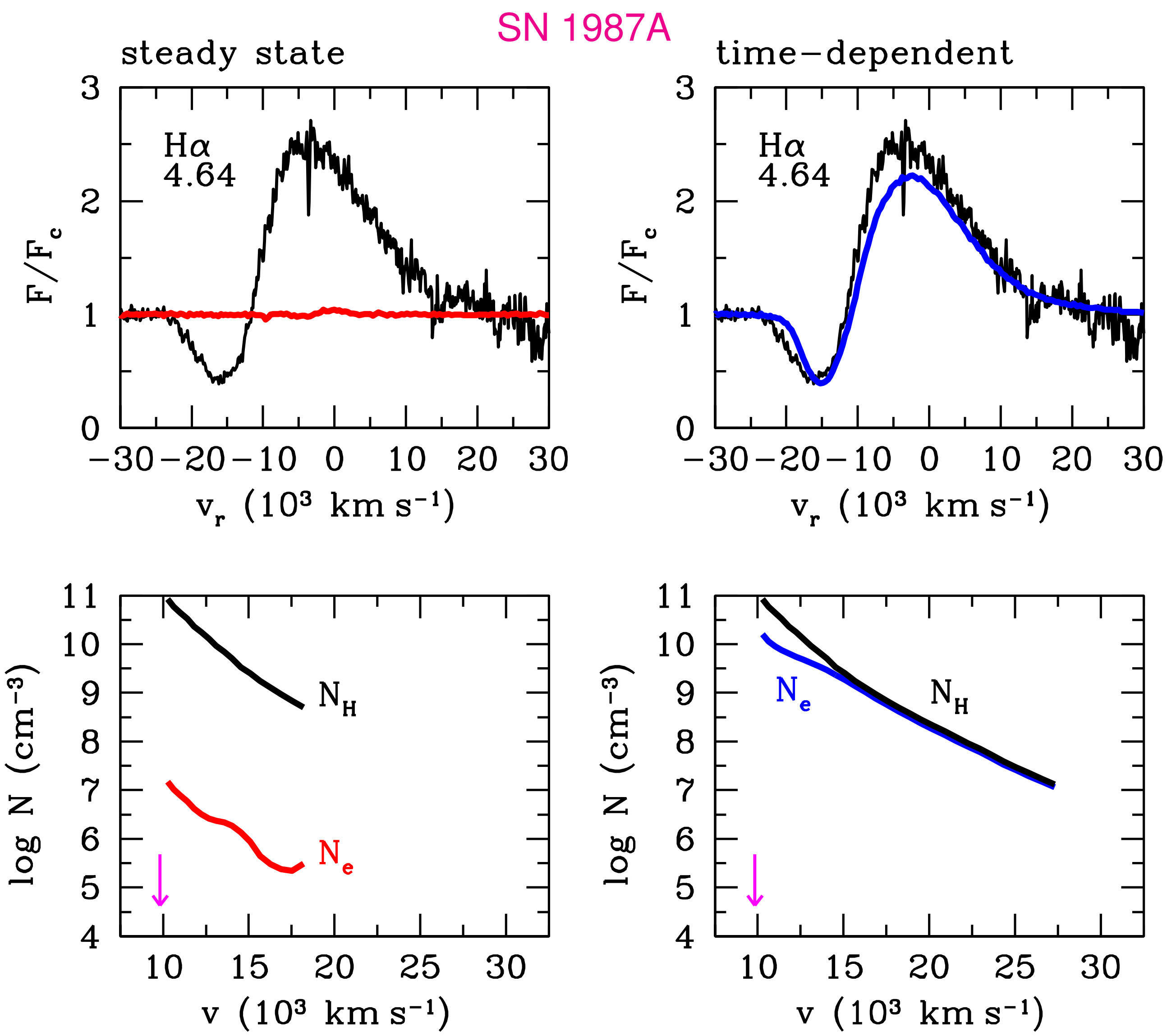

Hα and Hβ Lines Problem at Early Phase

The ratio $R_\tau = \tau_S(\mathrm{H}\alpha)/\tau_S(\mathrm{H}\beta)$ is determined by atomic data. Theoretical value is 7.25.

Ordinary type IIP SN 2008in: $R_\tau = 2.5$ (RSG)

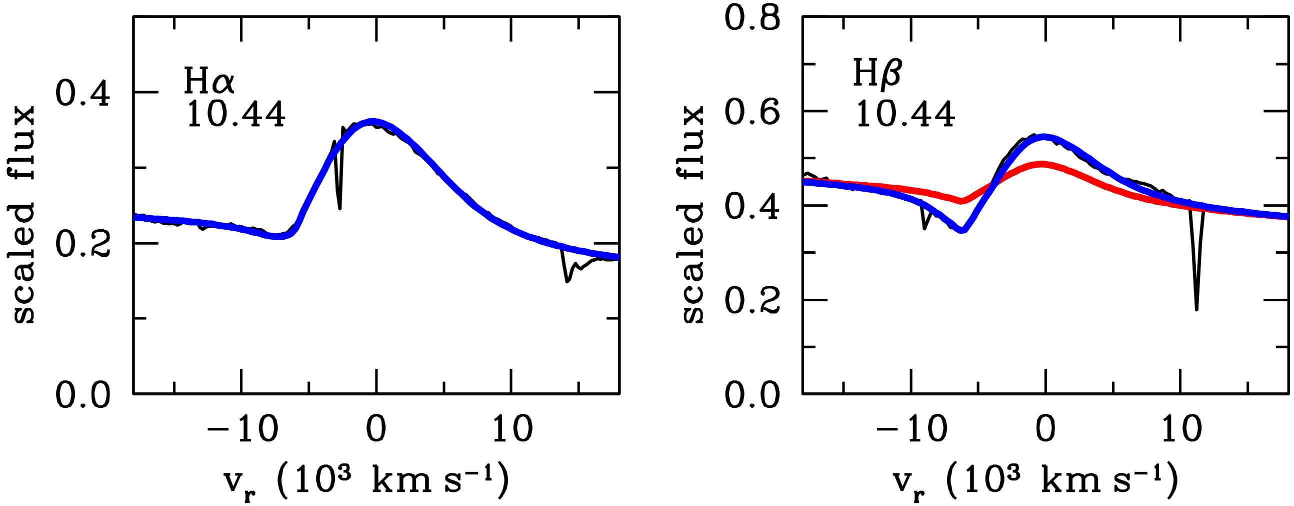

Peculiar type IIP SN 1987A: $R_\tau = 7.25$ (BSG)

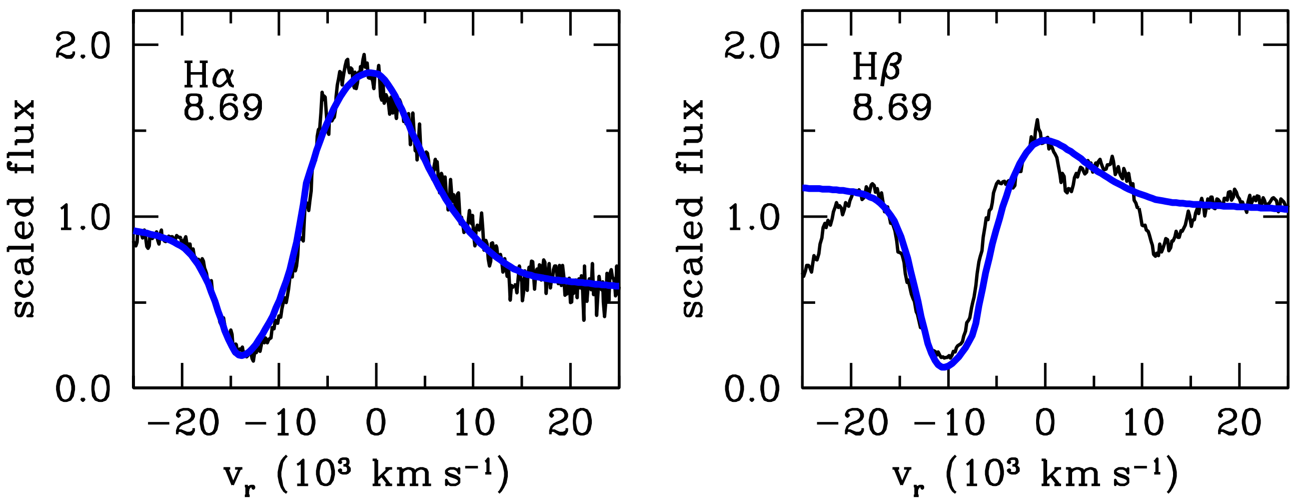

Inhomogeneous Outer Layers of Ejecta

Smooth medium

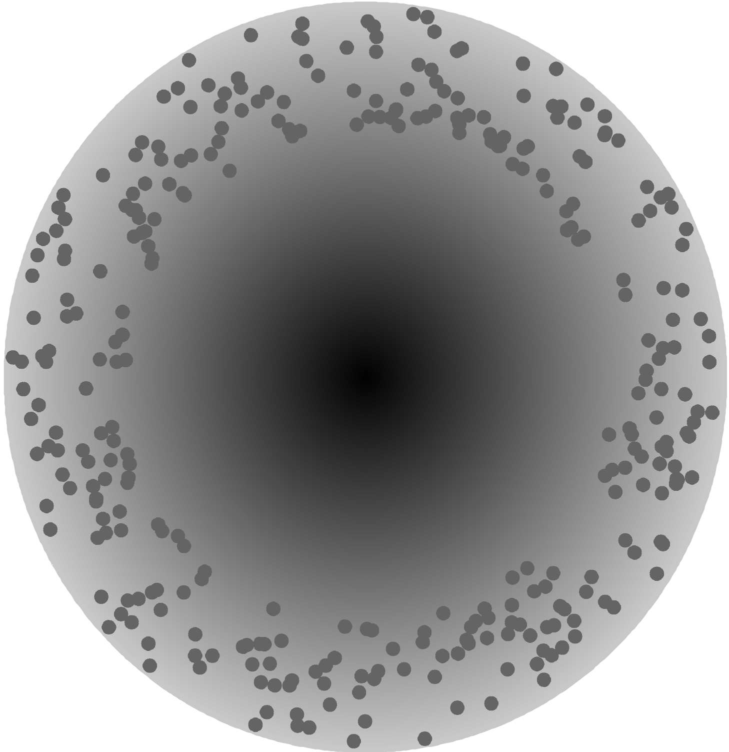

Clumpy medium

$$I_\nu = I_\nu^{ph} \left[f_c \exp\left(-\tau_c\right) + \left(1 - f_c\right) \exp\left(-\tau_{ic}\right) \right]$$

$$\nu = \nu_0 (1 - v_z/c)$$

$R_\tau = \tau_S(H\alpha)/\tau_S(H\beta) = 7.25$ both in clumps and interclump matter.

Clumping: Solution of Hα and Hβ Lines Problem

SN 2008in

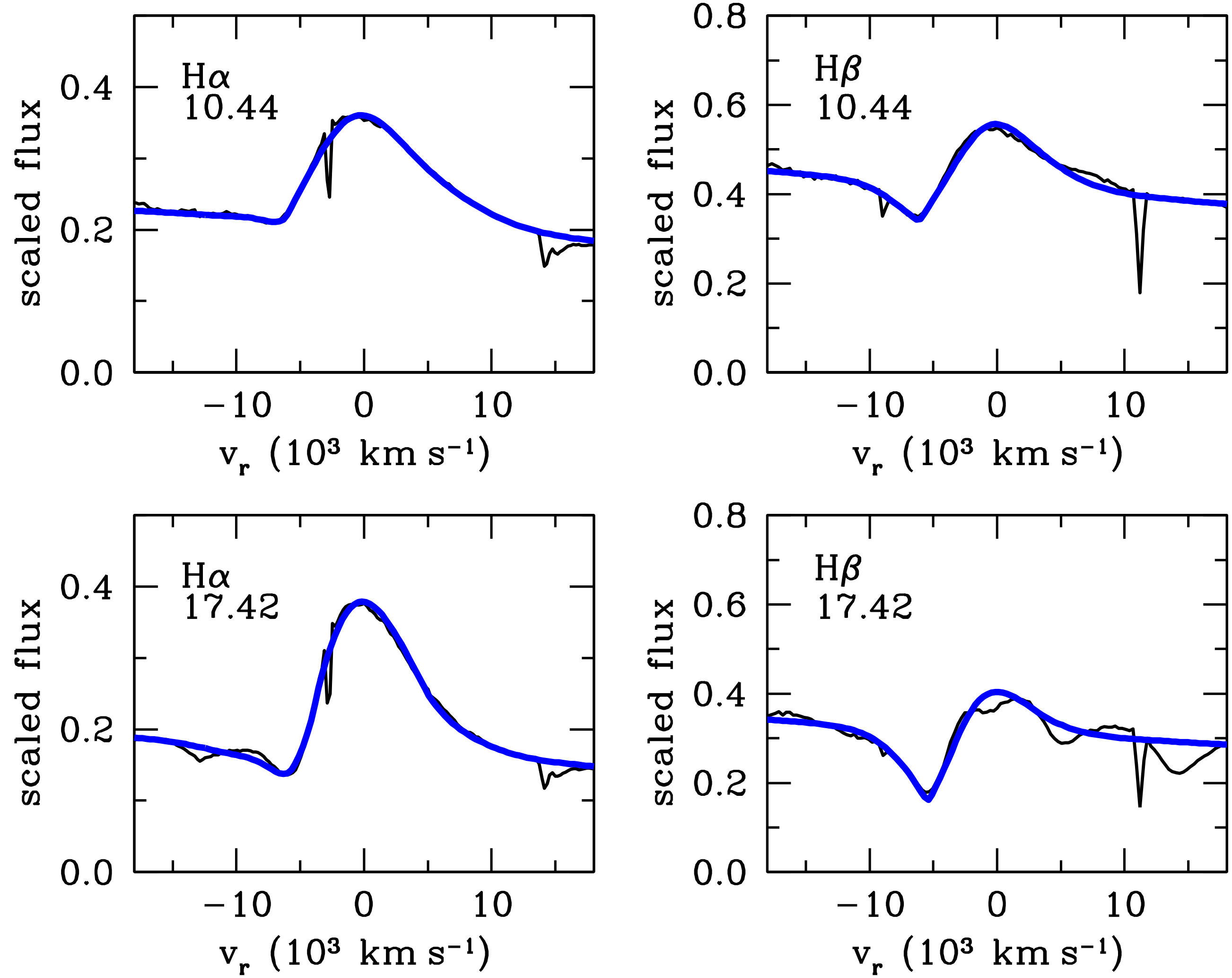

$f_c \approx 0.5$, $v_f \approx 6100\,\mathrm{km\,s^{-1}}$, $\tau_c \approx 100$, $\tau_{ic} \approx 1$, $M_f \approx 0.03\,M_\odot$ ($\sim 2 \times 10^{-3}$ of M_{env})

Origin of Clumps in Ordinary Type IIP Supernovae

RSG density profiles

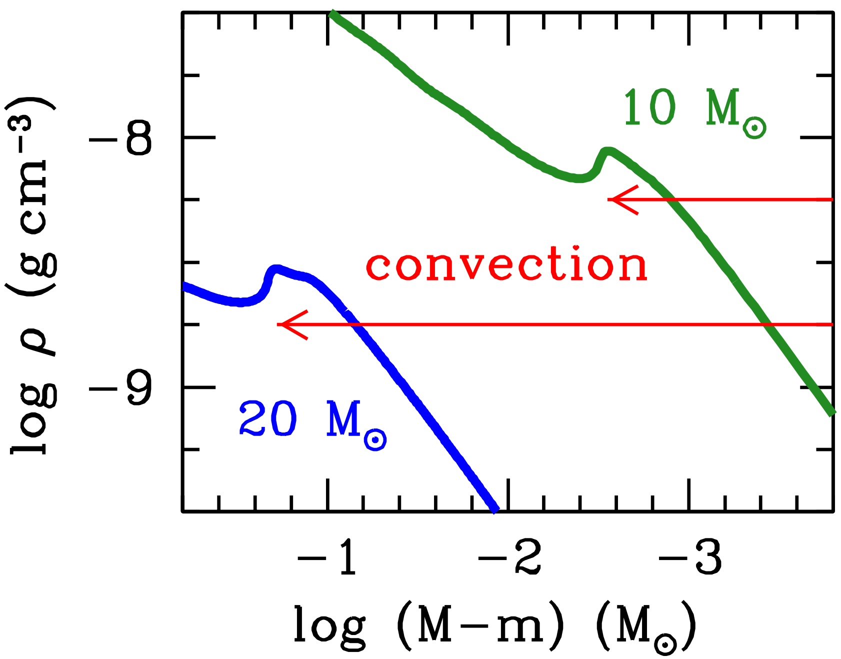

Fadeyev (2012)

Shock-turbulence interaction

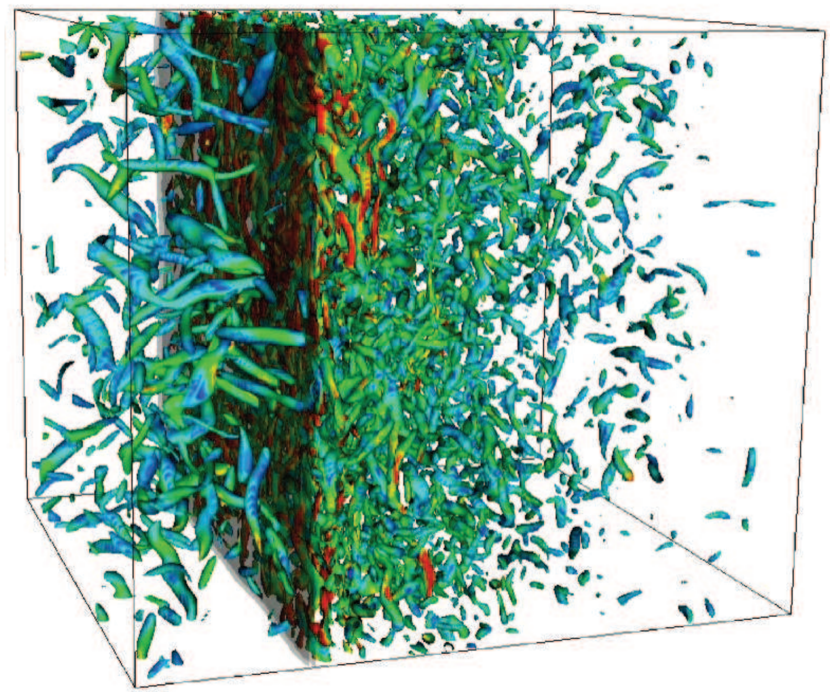

Lele et al. (2009)

Fundamentals of Clumping Description

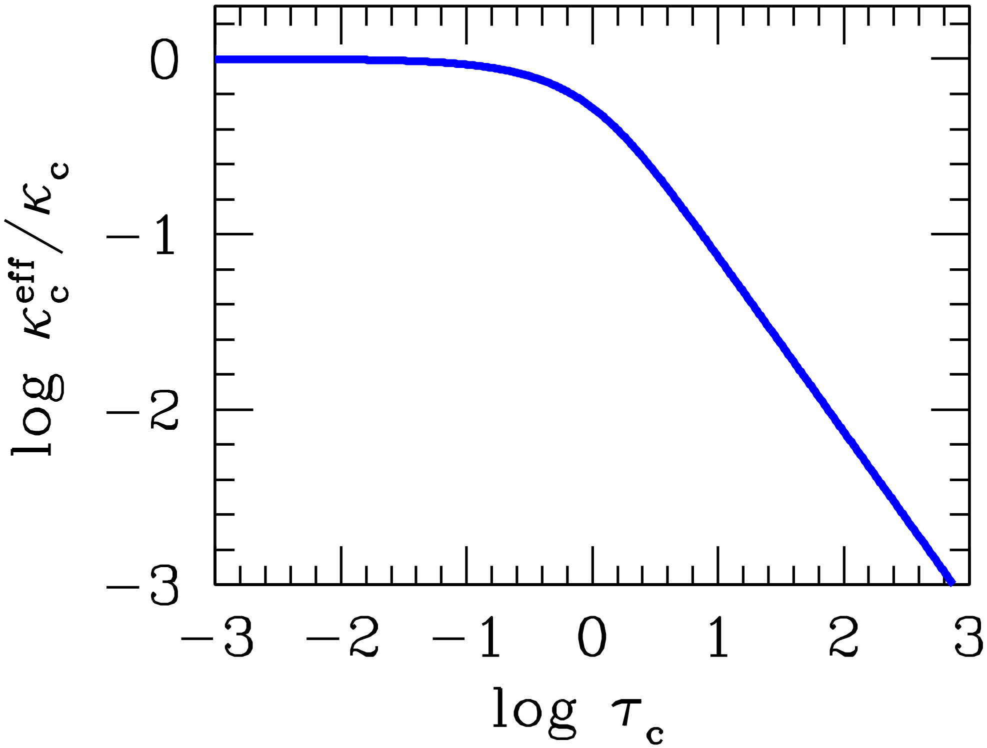

$$q(\tau_c) = \frac{3}{8\tau_c^3}\left[2\tau_c^2 - 1 + (1+2\tau_c)\exp(-2\tau_c)\right]$$

Basic Formulae

$$f_c = \mu_c D^{-1}$$

$$\rho_c = D\rho$$

$$\rho_{ic} = \frac{1-\mu_c}{1-f_c}\rho$$

$$k_{tot} = f_c k_c^{eff} + (1-f_c)k_{ic}$$

$$\eta_{tot} = f_c \eta_c^{eff} + (1-f_c)\eta_{ic}$$

$$k_c^{eff} = k_c\, q(\tau_c)$$

$$\eta_c^{eff} = \eta_c\, q(\tau_c)$$

Effects of Clumping in Hydrodynamic Modeling

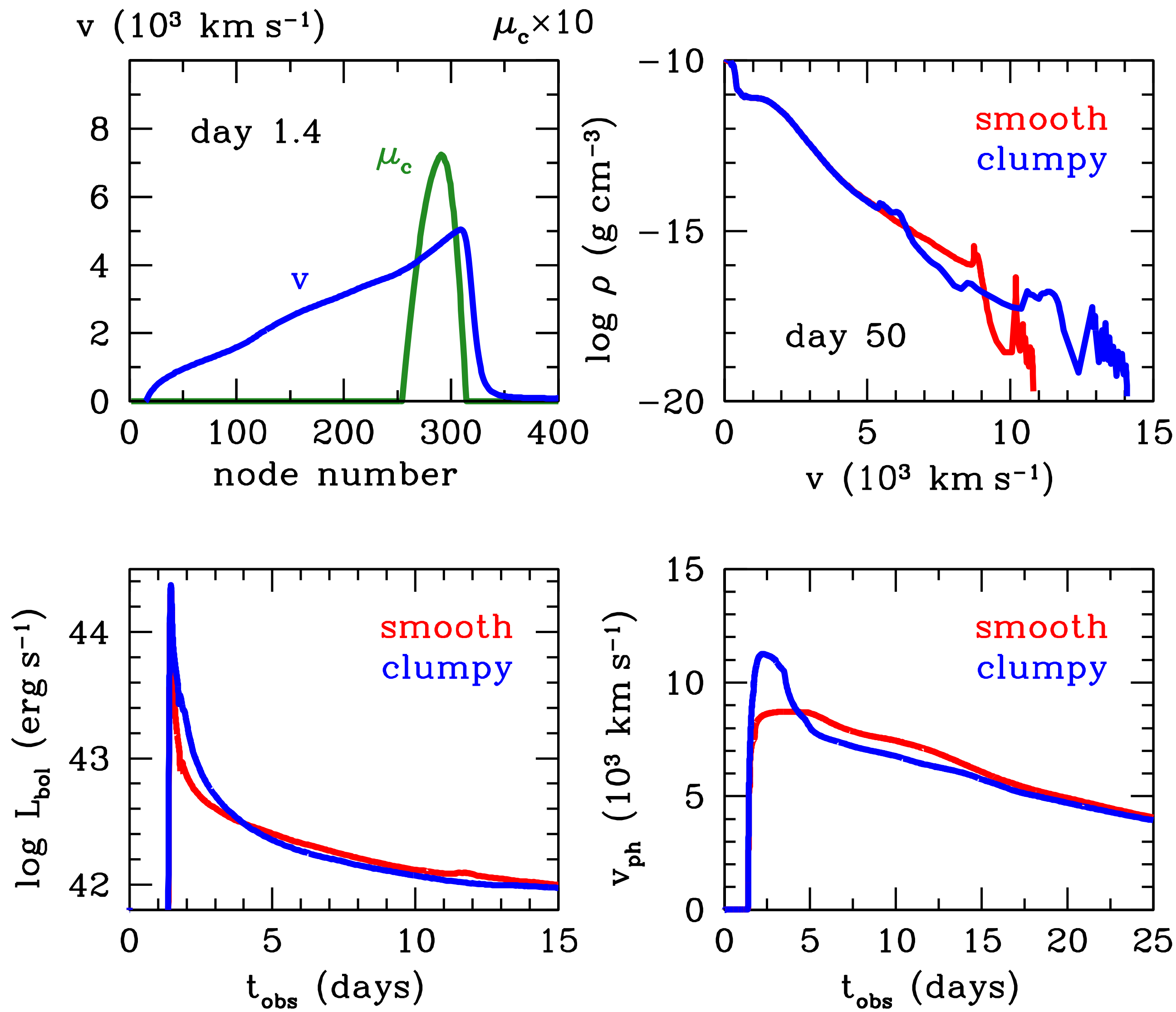

SN 2012A: $M_{\rm preSN} = 14.5 M_\odot$, clumpy mass $\sim 0.07 M_\odot$ with velocities > 5500 km s^{-1}.

Explosion Energy and ^{56}Ni Mass Versus Progenitor Mass

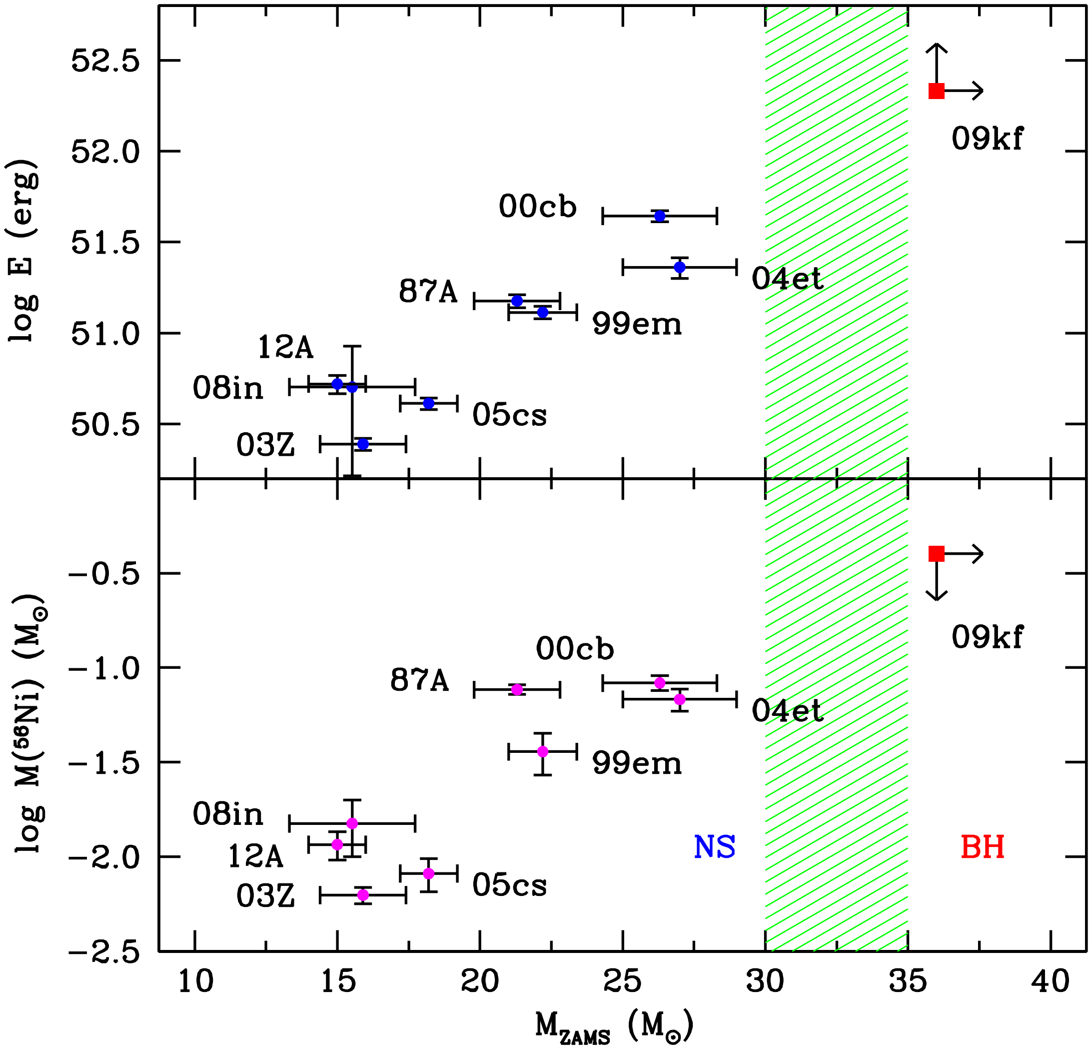

SN 2009kf

Single star scenario

2.2×10^{52} erg $\Rightarrow$ BH

NS/BH border in 30-35 $M_\odot$

"Missing" CCSNe

Extrapolated properties:

$M_{\rm ZAMS} \approx 10 M_\odot$

$E \approx 6 \times 10^{49}$ erg

$M_{\rm Ni} \approx 10^{-3} M_\odot$

Different Approach to Hydrodynamic Modeling

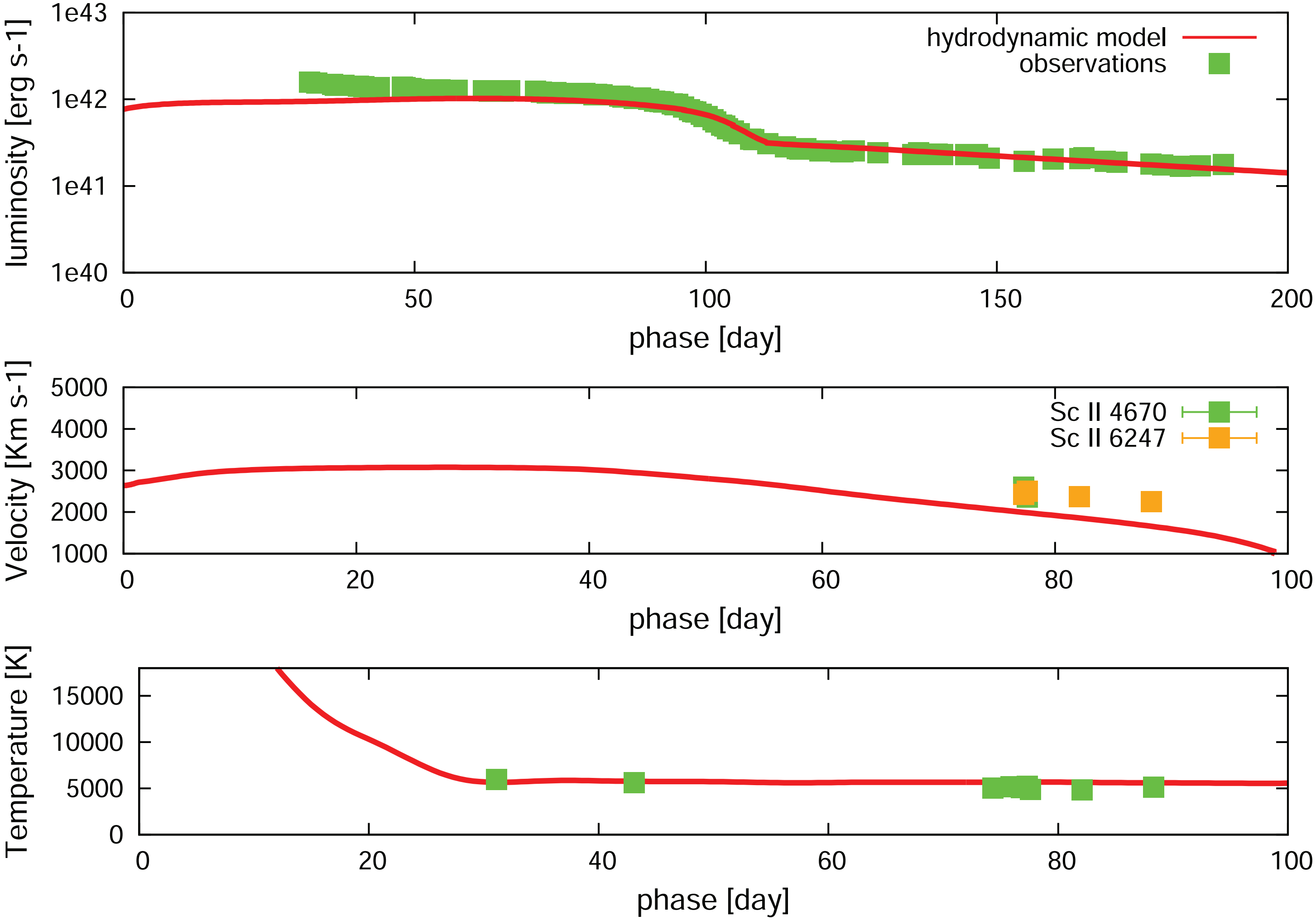

The best-fit model for SN 2013ab:

$R_0 = 603 R_\odot$, $M_{env} = 7 M_\odot$, $E = 0.35 \times 10^{51}$ erg (Bose et al. 2015).

SN 1987A: Evolutionary pre-SN models

Model	$R_{\rm pSN}$ $(R_\odot)$	$M_{\rm He}^{\rm core}$ $(M_\odot)$	$M_{\rm pSN}$ $(M_\odot)$	$M_{\rm ZAMS}$ $(M_\odot)$	$X_{\rm surf}$	$Y_{\rm surf}$	$Z_{\rm surf}$ (10^{-2})	$\xi_{1.5}$	Ref
B15	56.1	**4.05**	15.02	15.02	0.767	0.230	0.34	0.24	1
N20	47.9	**5.98**	16.27	$\sim$20.0	0.560	0.435	0.50	0.83	2
W18	46.8	**7.40**	16.92	18.0	0.480	0.515	0.50	0.68	3
W20	64.2	**5.79**	19.38	20.10	0.738	0.256	0.56	0.78	4

(1) Woosley et al. (1988);
(2) Shigeyama & Nomoto (1990);
(3) Woosley (2007);
(4) Woosley et al. (1997).

SN 1987A: Density distributions in the pre-SN models

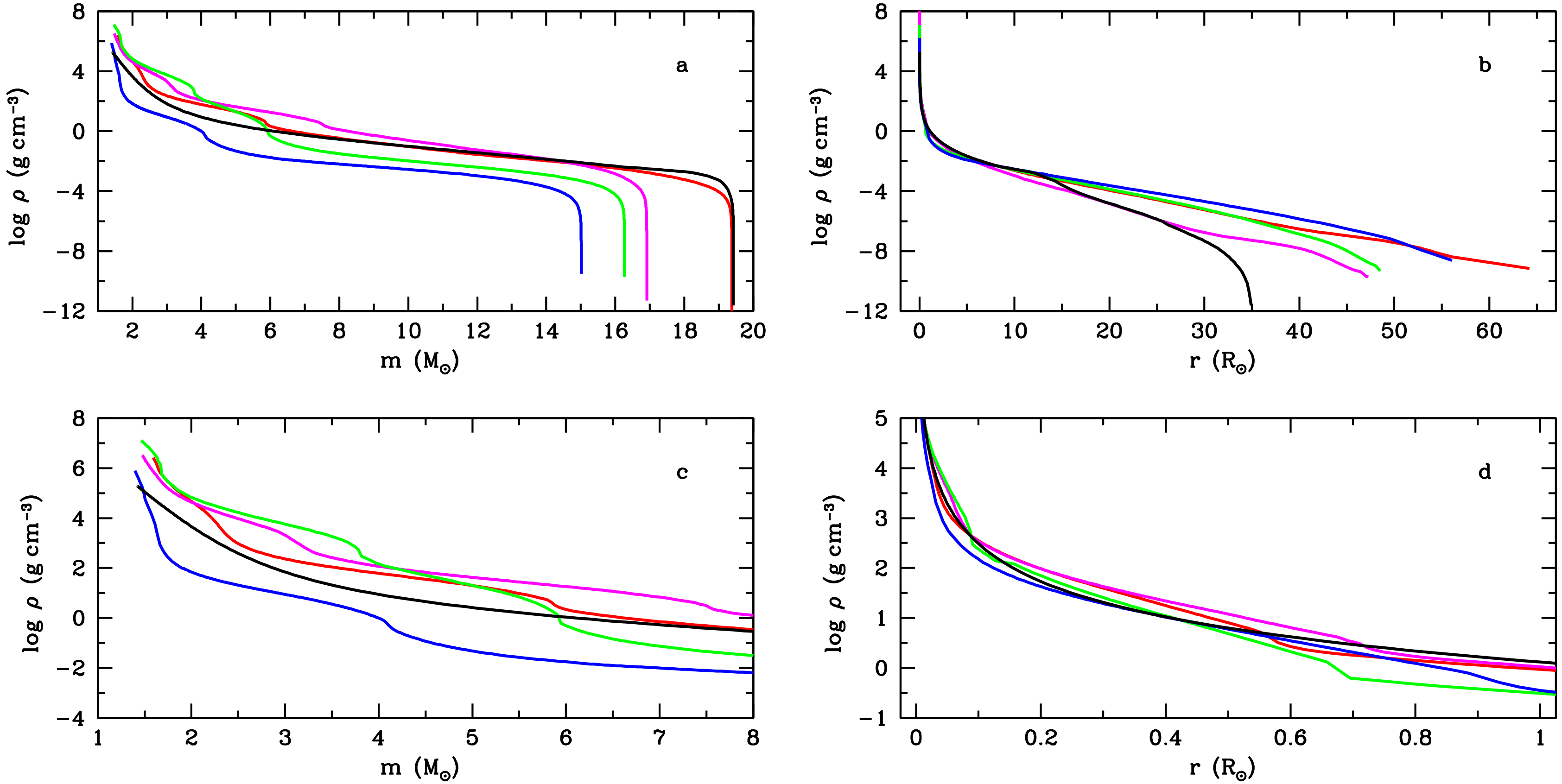

Models B15 (blue), N20 (green), W18 (magenta), W20 (red), and optimal model (black).

SN 1987A: Mass fractions in the pre-SN models

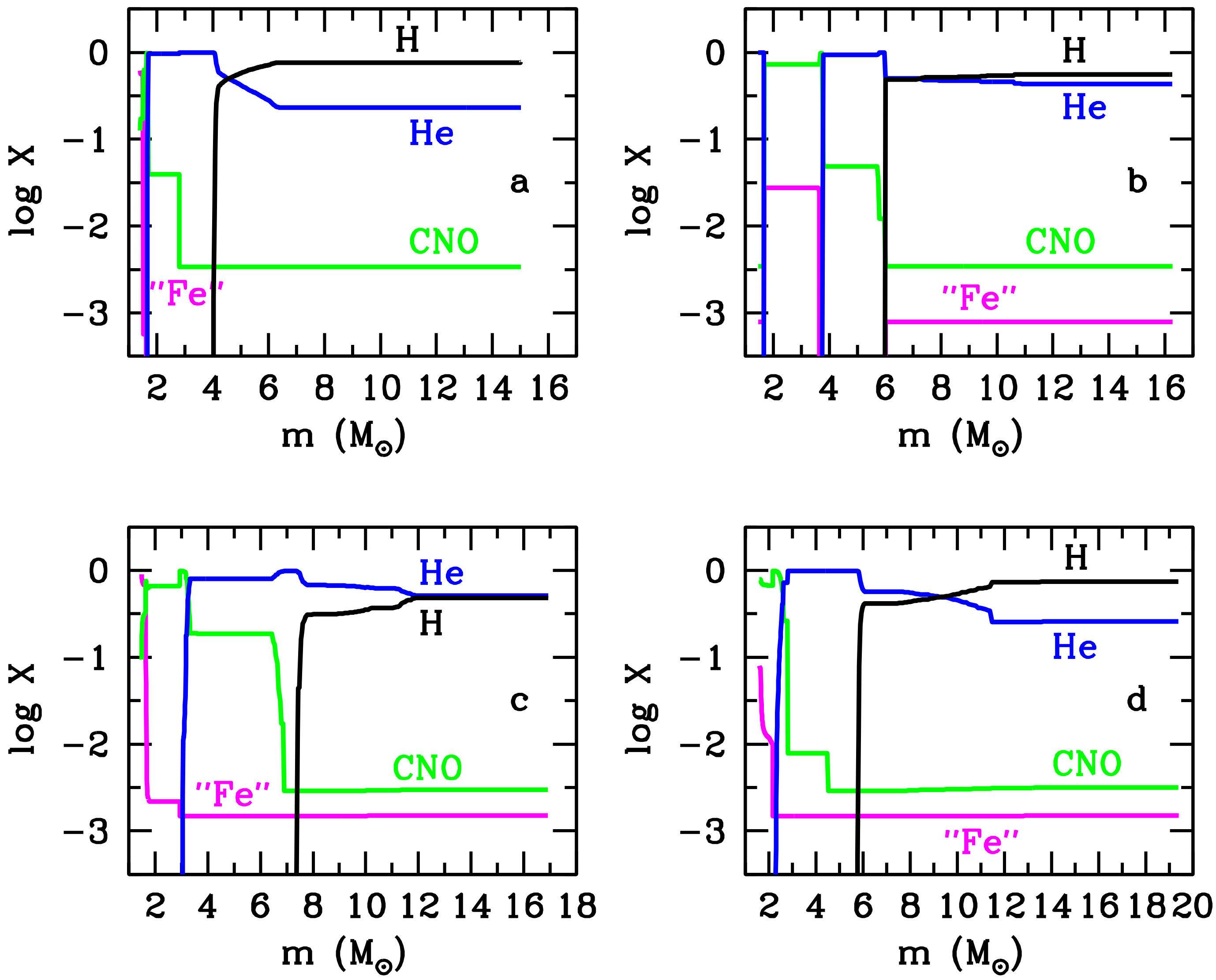

Models B15-2 (Panel **a**), N20-P (Panel **b**), W18 (Panel **c**), and W20 (Panel **d**).

SN 1987A: Morphology of radioactive ^{56}Ni-rich matter

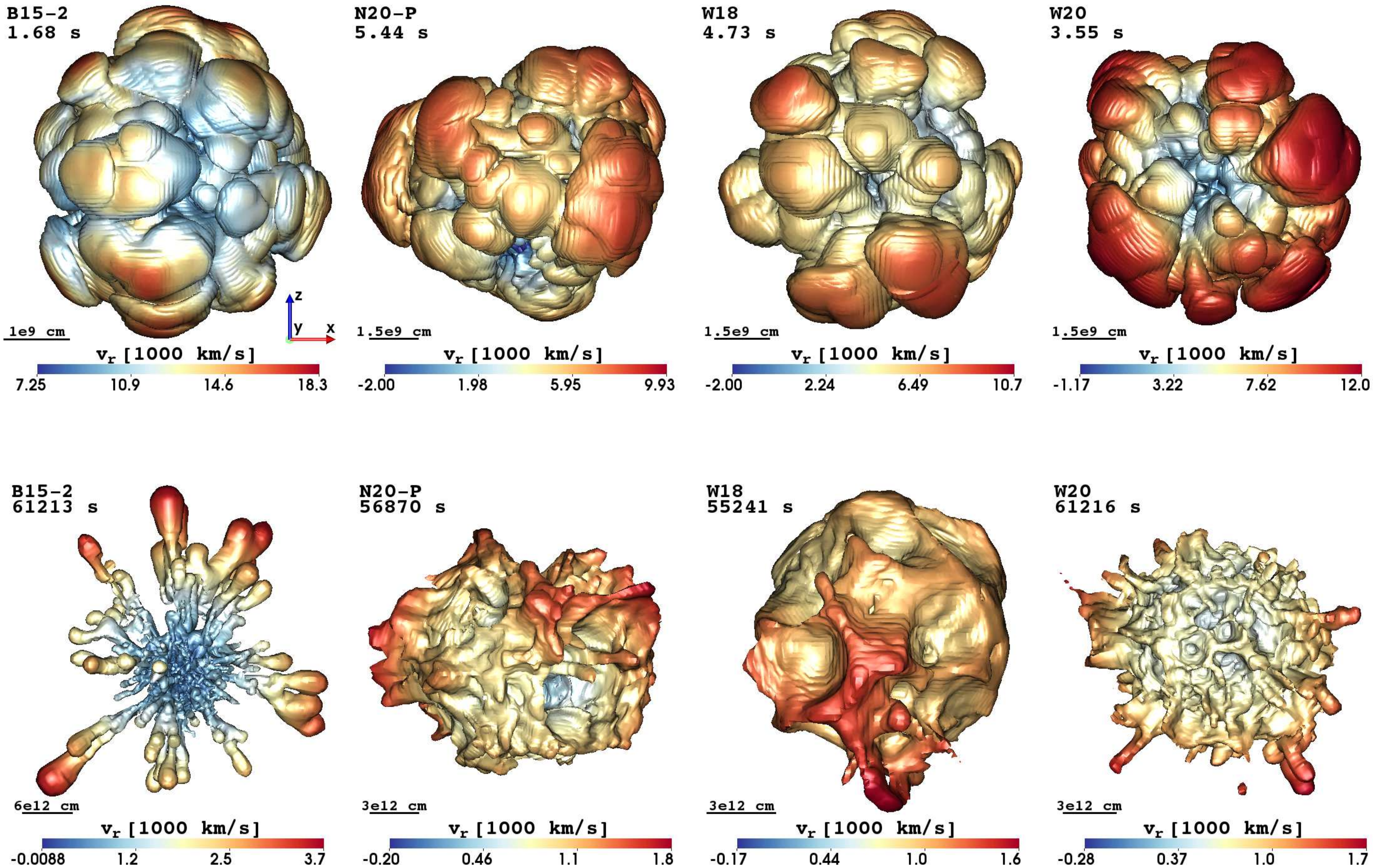

SN 1987A: Mass fractions as functions of velocity

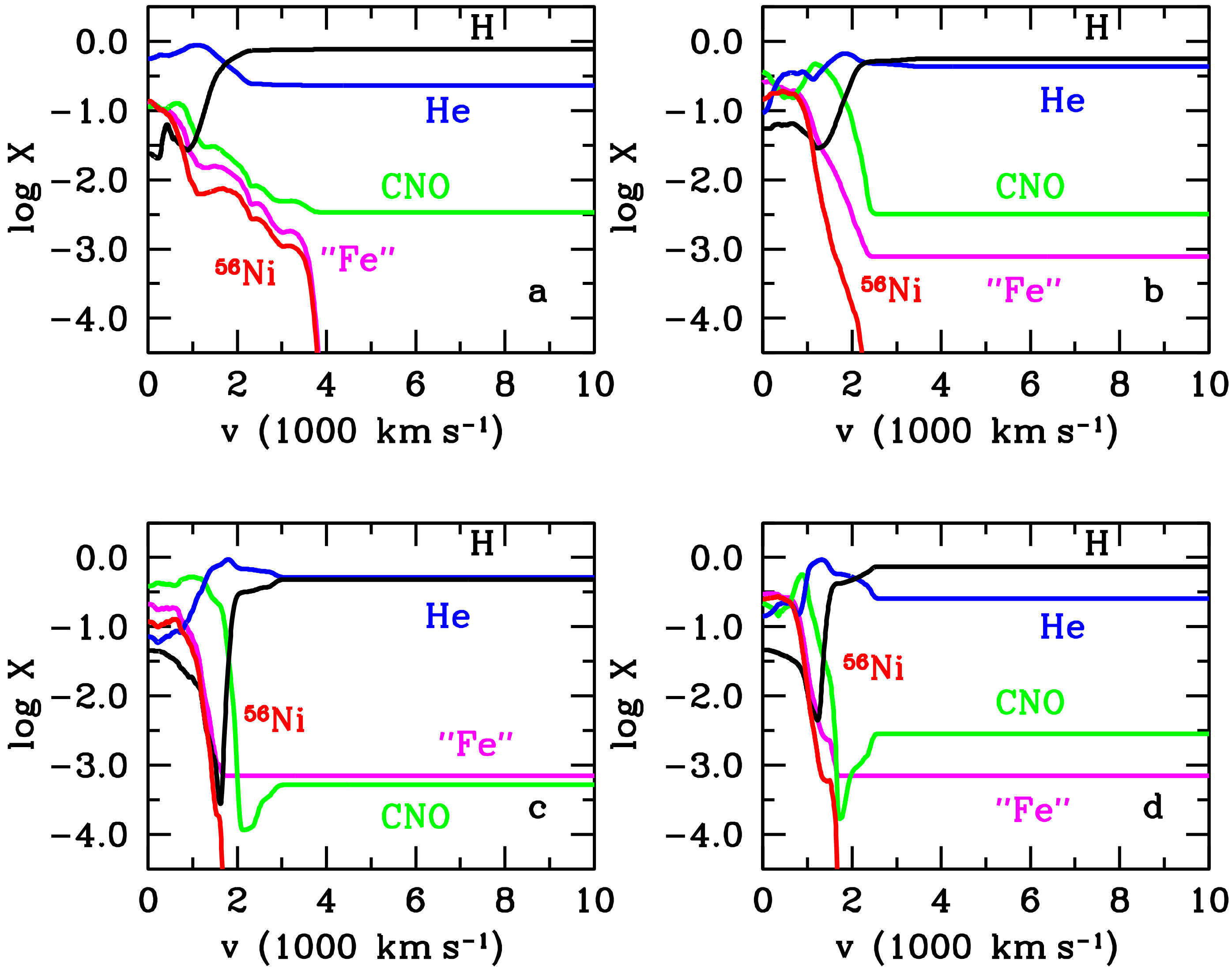

Models B15-2 (Panel **a**), N20-P (Panel **b**), W18 (Panel **c**), and W20 (Panel **d**).

SN 1987A: Bolometric light curves

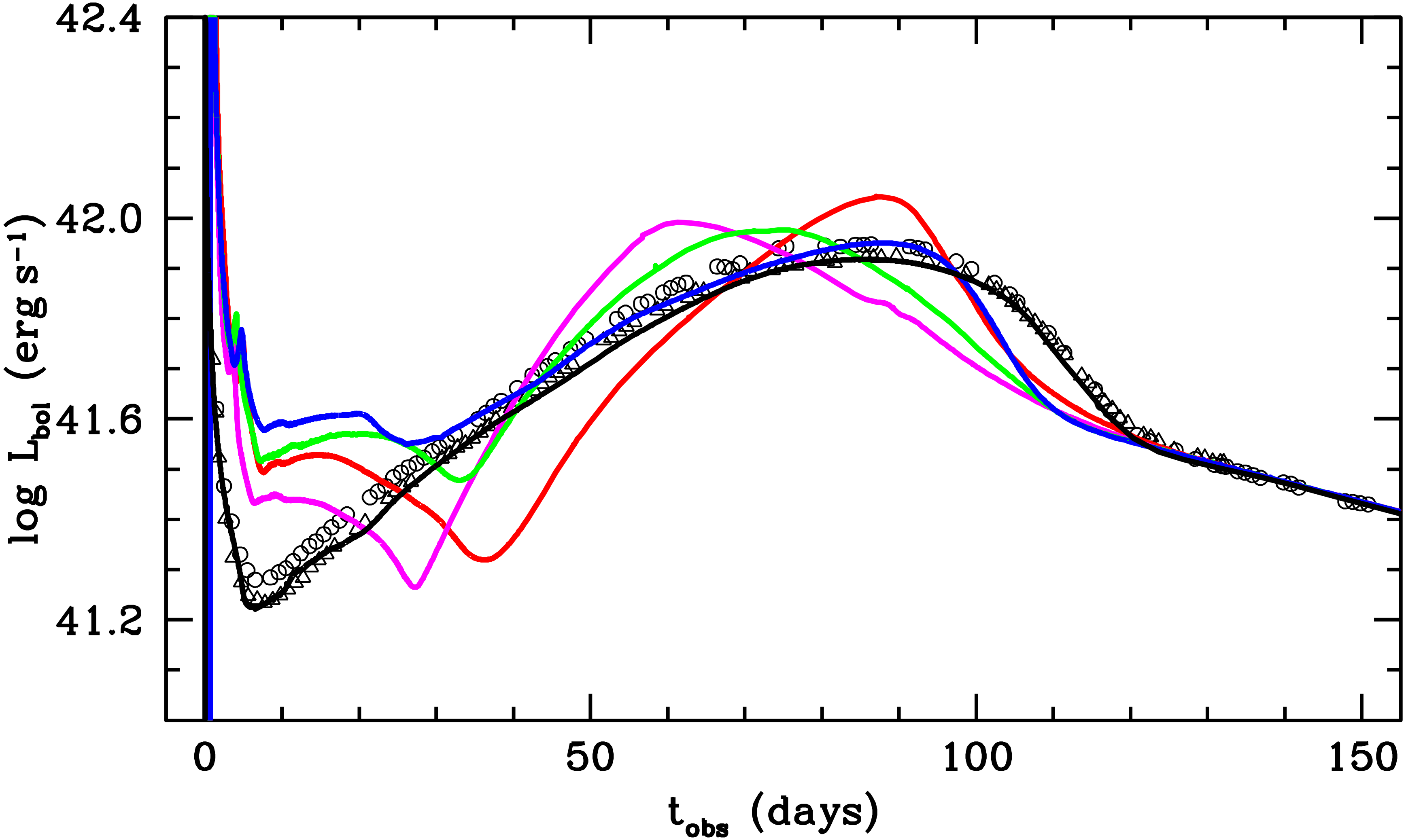

Models B15-2 (blue), N20-P (green), W18 (magenta), W20 (red), and optimal model (black).

Oxygen Doublet at Nebular Phase

$$\rho \propto M_e (vt)^{-3} \Rightarrow E \propto M_e^{5/3} \rho^{-2/3} t^{-2}$$

[OI] 6300, 6364 Å

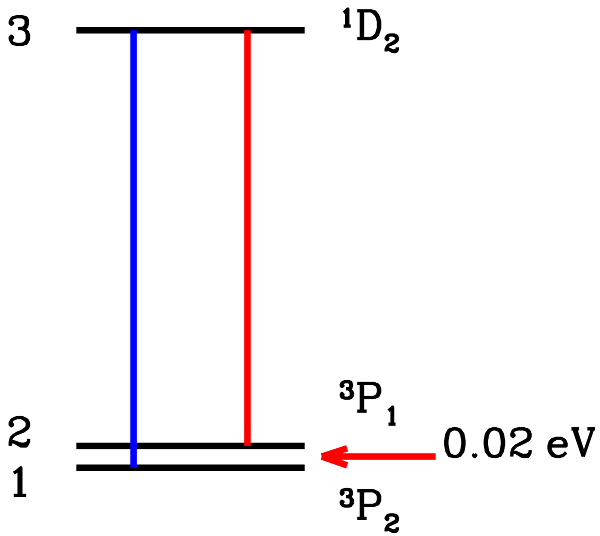

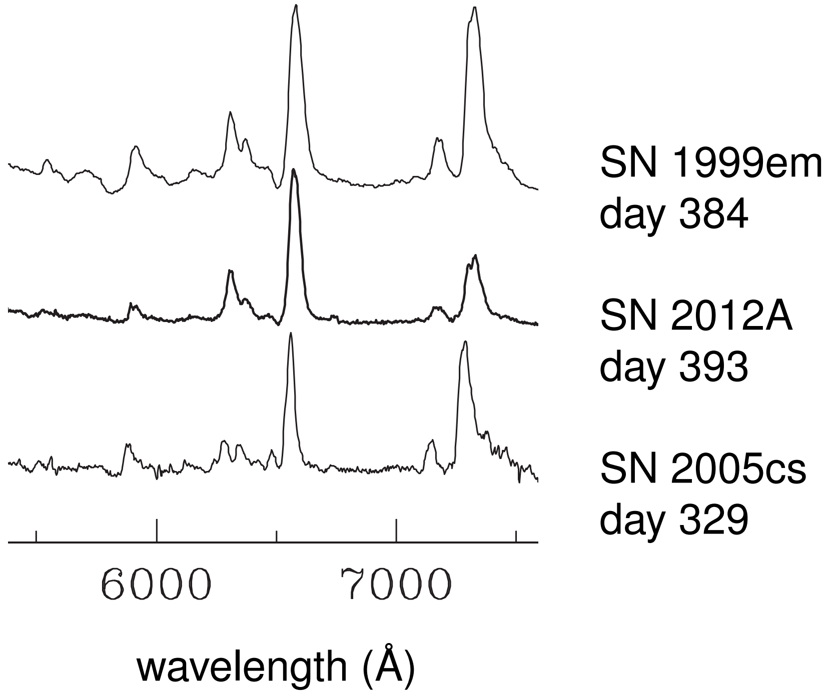

$$\frac{\text{Red}}{\text{Blue}} = \exp\left(E_{12}/kT\right) \left(\frac{\lambda_{13}}{\lambda_{23}}\right)^5 \frac{1-\exp\left(-\tau_{23}\right)}{1-\exp\left(-\tau_{13}\right)} \quad \Rightarrow \quad n(\mathrm{O})$$

$$\tau \propto n(\mathrm{OI})\, t, \quad n(\mathrm{O}) = n(\mathrm{OI})$$

Differential and Cumulative Density Distributions

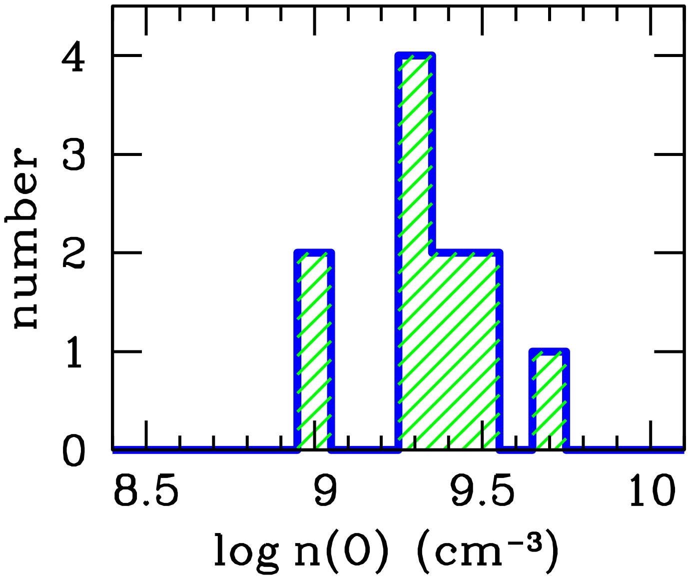

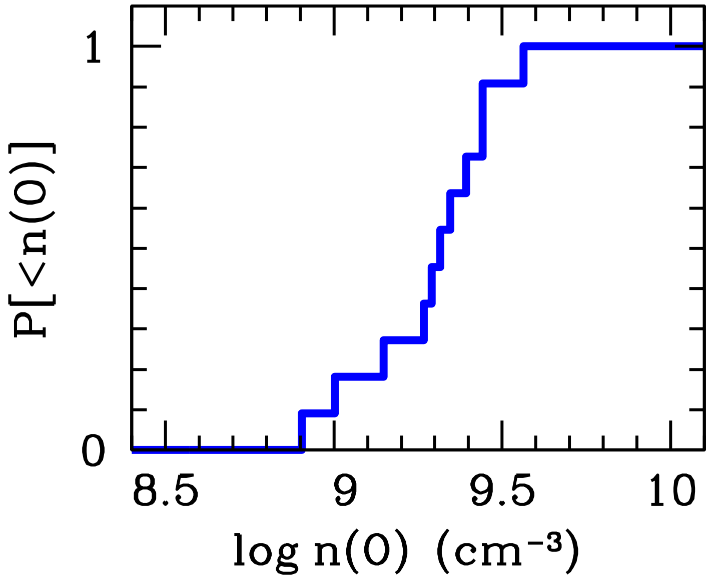

- The oxygen densities obtained for 11 SNe are reduced to day 300.
- The average value is 2.3×10^9 cm^{-3} with the standard deviation of 10^9 cm^{-3}.
- The found distributions do not depend on distance, extinction, or model assumptions.

Modeling Oxygen Density Distributions

$\rho \propto M_e(vt)^{-3} \Rightarrow E \propto M_e^{5/3}\rho^{-2/3}$ & $(2.3 \pm 1) \times 10^9$ cm^{-3} $\Rightarrow$ growing $E(M)$

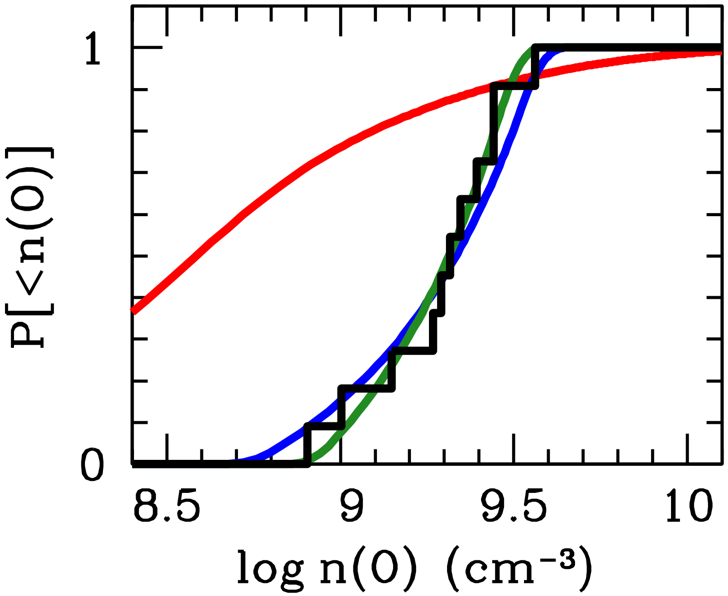

Model	M_1	M_2	E_1	E_2	k
	($M_\odot$)		(10^{51} erg)		
Model 1*	9	25	0.2	4	–
Model 2	9	25	0.2	4	2.9
Model 3	9	20	0.2	2	2.9

* No correlation between E and M.

$E \propto M^k$
$k = \ln(E_2/E_1)/\ln(M_2/M_1)$

- Progenitor mass M: Salpeter law $dN/dM \propto M^{-2.35}$ in the range $M_1 < M < M_2$.
- Explosion energy E: relation $E = E_1(M/M_1)^k$ in the range $E/s - sE$, $s = 1.1$.
- Ejecta: $\rho = \rho_0/(1 + (v/v_0)^q)$, v_0 and ρ_0 are determined by E and M_e, and $q \approx 8$.

Empirical and Hydrodynamic Energy-Mass Relations